HHS Public Access

Author manuscript

Nat Neurosci. Author manuscript; available in PMC 2014 August 01.

Published in final edited form as:

Nat Neurosci. 2014 February ; 17(2): 262–268. doi:10.1038/nn.3627.

Imaging an optogenetic pH sensor reveals that protons mediate lateral inhibition in the retina

Tzu-Ming Wang[1], **Lars C. Holzhausen**[1], and **Richard H. Kramer**[1]

[1]Department of Molecular and Cell Biology, University of California, Berkeley

Abstract

The reciprocal synapse between photoreceptors and horizontal cells (HCs) underlies lateral inhibition and establishes the antagonistic center-surround receptive fields of retinal neurons, to enhance visual contrast. Despite decades of study, the signal mediating negative feedback from HCs to cones has remained controversial because the small, invaginated synaptic cleft has precluded measurement. Using zebrafish retinas, we show that light elicits a change in synaptic proton concentration with the correct magnitude, kinetics and spatial dependence to account for lateral inhibition. Light, which hyperpolarizes HCs, causes synaptic alkalinization, whereas activating an exogenously expressed ligand-gated Na^+ channel, which depolarizes HCs, causes synaptic acidification. While acidification was prevented by blocking a proton pump, re-alkalinization was prevented by blocking proton-permeant ion channels, suggesting that distinct mechanisms underlie proton efflux and influx. These findings reveal that protons mediate lateral inhibition in the retina, raising the possibility that protons are unrecognized retrograde messengers elsewhere in the nervous system.

INTRODUCTION

Lateral inhibition is a key neural network phenomenon that enhances contrast sensitivity in nearly every sensory system. As the first laterally projecting neuron in the retina, horizontal cells (HCs) initiate lateral inhibition in the visual system[1], but the synaptic mechanism involved in this process is still unclear. We know that photoreceptors continuously release the neurotransmitter glutamate in darkness to depolarize HCs[2]. HCs, in turn, transmit a negative feedback signal that inhibits activation of voltage-gated Ca^{2+} channels in the photoreceptor terminals[3,4], thereby reducing Ca^{2+}-dependent glutamate release. However, the identity of the negative feedback signal has remained uncertain.

Correspondence and requests for materials should be addressed to: R.H.K. (rhkramer@berkeley.edu)., 121 Life Sciences Addition, Berkeley, CA 94720, USA.

Author contributions

T.M.W. and R.H.K conceived the project. T.M.W. performed most of the experiments, analyzed the data, and developed plugins for the image acquisition software. L.C.H. made the FaNaC and the double transgenic fish lines, collected and analyzed the electrophysiological data, and prepared Fig. 6a and Supplementary Fig. 4. T.M.W. and R.H.K. prepared the manuscript, and all authors edited the manuscript.

The authors declare no competing financial interests.

For many years, the inhibitory neurotransmitter GABA was thought to mediate negative feedback. Early studies showed that HCs release GABA upon depolarization[5] and cones possess GABA receptors[6]. However, later studies showed that a wide variety of GABA receptor antagonists fail to alter negative feedback or lateral inhibition[7,8]. Moreover, there is no evidence that the concentration of GABA in the synaptic cleft changes during illumination to account for lateral inhibition.

As an alternative, an ephaptic mechanism of negative feedback was proposed[9,10]. In this scenario, depolarization of HCs causes current to flow through open channels located in the tips of HC dendrites, which extend into the invaginated cone terminal. This current leads to an increase of extracellular potential, which has the same effect as intracellular hyperpolarization, is sensed by voltage-gated Ca^{2+} channels in the cone terminal, altering Ca^{2+} influx and Ca^{2+}-dependent glutamate release. Hemichannels are found to be concentrated in the dendritic tips of HCs in fish[10,11], making them a candidate for transmitting the putative ephaptic signal from HCs to cones. However, while modeling studies support the possibility of ephaptic signaling, there has been no direct experimental evidence that a local change in extracellular potential actually occurs during lateral inhibition.

Finally, protons have been proposed as the negative feedback transmitter. In this scenario, illumination hyperpolarizes HCs which decreases proton efflux. The resulting change in extracellular pH modulates the voltage-dependent gating of cone Ca^{2+} channels, with alkalinization allowing the channels to open at a more negative membrane potential. The alkalinization is a “negative feedback” effect because it increases cone release, opposite to the direct effect of light on cones, which decreases release. Negative feedback and lateral inhibition can be blocked by adding a high concentration of exogenous pH buffer, consistent with the proton hypothesis (for review, see Ref. 12). However, some of these buffers may acidify the intracellular pH and affect hemichannels, raising concerns about the mechanism of their blockade[13]. And as is the case for the other putative signals, there has been no direct evidence demonstrating a light-dependent change in proton concentration in the synaptic cleft.

Extracellular pH can be measured with pH-sensitive microelectrodes, but these are too blunt and invasive for accurate measurements in the synaptic cleft. Measurements can be made with pH indicator dyes, but their spatial resolution is inadequate for accurate synaptic localization of the signal. Hence, to provide a reliable and accurate measure of pH precisely in the synaptic cleft, we engineered a genetically-encoded pH indicator expressed on the plasma membrane of the cone terminal. We fused a pH-sensitive form of GFP (pHluorin)[14] onto the extracellular side of a subunit of the cone Ca^{2+} channel. Hence the pH indicator is on the same channel that normally serves as the effector of negative feedback. Using this optogenetic pH indicator we observed a light-elicited change in fluorescence intensity that indicates a change in synaptic pH. Moreover, the signal has the appropriate magnitude, direction, and spatial dependence to account for at least most of the negative feedback signal underlying lateral inhibition.

RESULTS

CalipHluorin: A genetically encoded reporter of synaptic pH

To detect changes in pH at the invaginating synapse of cones, we fused superecliptic pHluorin onto the N-terminus of the α2δ4 subunit of the L-type Ca^{2+} channel, and we named the resulting fusion protein CalipHluorin (Fig. 1a,b). To determine whether CalipHluorin can report changes in pH we first expressed the protein in cultured rat hippocampal neurons and measured fluorescence while superfusing solutions buffered to different values of pH. Fluorescence dropped rapidly upon acidifying extracellular pH (Supplementary Fig. 1), as observed with other pHluorin constructs expressed on the cell surface[14].

To confirm that the response to pH was mediated by CalipHluorin on the cell surface rather than in internal organelles, a thrombin proteolytic cleavage site was inserted between the extracellular pHluorin region and the membrane-spanning α2δ4 region. Thrombin treatment of cells expressing this construct resulted in removal of cell surface fluorescence and elimination of the response to acidification (Supplementary Fig. 1). Hence the pH response must be attributed to cell surface CalipHluorin.

We then generated a transgenic zebrafish line expressing CalipHluorin in cones, driven by the cone transducin-α promoter[15]. We found that some CalipHluorin was expressed at the soma of cones (Fig. 1c–e). However, its fluorescence was particularly concentrated in puncta in cone terminals (Fig. 1c,f,g) which are known to possess clusters of voltage-gated Ca^{2+} channels adjacent to vesicular release sites near synaptic ribbons[16]. We observed that the line of zebrafish generated in this study had CalipHluorin expression that was highest in the UV- and blue-sensitive cones (Fig. 1e,f), which can be identified by their characteristic sizes and repeating pattern in the retina[17].

Light induces alkalinization of the cone synaptic cleft

To optically measure changes in synaptic pH in response to light, we imaged CalipHluorin in flat-mounted retina. Images were obtained with a series of 910 nm laser scans repeated at a constant rate (~8 Hz) throughout the experiment. Repeated two-photon scanning with infrared light results in some degree of light adaptation, but the retina can still generate robust responses to bright stimulus light[18]. Hence in the midst of the scan series, we stimulated photoreceptors with a flash of bright light (Fig. 2a). Comparison of images revealed that CalipHluorin fluorescence at cone terminals was brighter immediately after the flash and gradually returned to baseline within 0.5 s after a 0.5 s flash (Fig. 2b,c). On average, terminals exhibited a 5% increase in fluorescence intensity immediately after light stimulation (mean ± SEM: 1.051 ± 0.008, $n = 23$; Fig. 2c). The fluorescence increase indicates that the synaptic cleft was alkalinized during the light flash, which should allow Ca^{2+} channels to open at more negative membrane potential[19,20]. The change in fluorescence was observed in synaptic terminals but not in the soma of cones (1.003 ± 0.003, $n = 20$, $p = 1.7*10^{-6}$; Fig. 2c). Furthermore it was blocked by substituting the weak pH buffer bicarbonate with 20 mM of the strong pH buffer HEPES (0.996 ± 0.004, $n = 21$, $p = 2.7*10^{-7}$; Fig. 2c) and the non-aminosulfonate buffer Tris (1.005 ± 0.003, $n = 21$, $p =$

$4*10^{-6}$; Supplementary Fig. 2c). Hence light, which hyperpolarizes HCs in the retina, alkalinizes the synaptic cleft selectively.

Quantification of the light-induced pH change

To quantify the light-elicited pH change, we calibrated the relationship between pH and fluorescence intensity. We superfused solutions with different pH values on CalipHluorin-expressing cone terminals in a retinal slice, a preparation that allows faster equilibration of buffer solutions than a retinal flat-mount. Increasing the pH caused an increase in CalipHluorin fluorescence and decreasing pH caused a decrease (Fig. 3a). From the fitted titration curve (Fig. 3b), we estimate that the pKa of CalipHluorin is 6.9 and the pH at cone terminals in darkness is about 7.4 (n = 4 retinas). Using this dark value as a starting point, we stepped the pH from 7.4 to 7.6 (Fig. 3c) and estimated that the alkalinization required to elicit a 5% increase of fluorescence from the pH in the dark is 0.14 ± 0.01 pH units (n = 6 retinas). Previous studies have shown that alkalinization of 0.1 pH unit hyperpolarizes the mid-point of voltage-dependent gating of cone Ca^{2+} channels by 1–3 mV[20,21]. Superimposing diffuse full-field illumination on a central spot induced a steady-state shift of Ca^{2+} channel gating of 1.8–4 mV[19]. Therefore, the magnitude of the light-induced alkalinization is in the correct range to account for the steady-state effects of lateral inhibition by surround illumination.

Temporal and spatial features of the CalipHluorin response

The magnitude of the CalipHluorin signal increased with flash duration up to about 200 ms (Fig. 4a). This indicates that the pH in the synaptic cleft had reached equilibrium by this time. With a shorter light flash, the peak signal was smaller and delayed, occurring after the return to darkness (50 ms, Fig. 4b). These kinetics are similar to the time course of membrane potential responses in fish HCs to different duration light flashes[22].

The light intensity requirements and spatial response properties of the CalipHluorin signal are also in agreement with those of the HC light response. The CalipHluorin signal increased steeply with increasing stimulus intensity and saturated in bright light (Fig. 5a), consistent with the dynamic range of HCs in the fish retina[23]. The CalipHluorin response was dependent on spatial integration of light responses over a broad area of the retina. When we imaged a group of cone terminals and projected a small circular spot of light (50 μm diameter) that barely covered the imaged area (30 μm-by-30 μm square), the stimulus light produced little or no significant change in the CalipHluorin signal (1.008 ± 0.003, n = 27). However, when the spot diameter was expanded to illuminate more of the surround, the signal grew larger and reached a maximum with a spot diameter of 0.5 – 1 mm, well beyond the borders of the imaged area itself (Fig. 5b). This spot diameter falls within the range of the receptive field sizes of HCs in fish retina[24]. Moreover, an annulus of light with a dark center covering all of the imaged area (inner diameter = 300 μm, outer diameter = 1 mm) also elicited a significant increase in the CalipHluorin signal (1.032 ± 0.005, n = 20, p = $9.1*10^{-5}$; Fig. 5c). Hence the CalipHluorin response is generated by laterally-projecting neurons that have receptive field properties identical to HCs.

Blocking synaptic transmission prevents the CalipHluorin response

Synaptic transmission of the light response to HCs relies on presynaptic voltage-gated Ca^{2+} channels in photoreceptors and postsynaptic AMPA receptors in HCs. To test the involvement of Ca^{2+} channels in the CalipHluorin response, we used the L-type Ca^{2+} channel antagonist nifedipine. Nifedipine (100 μM) reduced the light-elicited CalipHluorin response by ~40% (1.031 ± 0.006, n = 25, p = 0.038; Fig. 5d), similar to the fraction of Ca^{2+} current inhibited in cones (~50% in slices[25]).

We next tested whether blocking negative feedback also prevents the CalipHluorin response. We found that the CalipHluorin response was also blocked by DNQX (150 μM, 1.001 ± 0.005, n = 21, $p = 2.1*10^{-6}$) or GYKI-52466 (50 μM, 1.008 ± 0.004, n = 21, $p = 1.3*10^{-5}$), which are competitive and non-competitive AMPA receptor antagonists, respectively (Fig. 5d and Supplementary Fig. 2d). AMPA receptors are absent from photoreceptors[26,27], hence the CalipHluorin response is not cone-autonomous. Taken together, the spatial, temporal, and pharmacological properties of the CalipHluorin response are consistent with mediation by HCs.

While HCs appear to be the primary source of the light-elicited CalipHluorin signal, events intrinsic to cones can also lead to changes in synaptic pH. Synaptic vesicles are acidic, and patch clamp recordings from cones indicate that phasic exocytosis can lower the pH near release sites, transiently inhibiting nearby cone voltage-gated Ca^{2+} channels[20]. We noticed that at the initial relaxation rate of the light-elicited CalipHluorin signal is smaller than predicted from exponential decay of synaptic alkalinization (see Fig. 4c, gray). This deviation might be a consequence of the transient acidification caused by vesicular protons.

To detect the transient acidification at light offset we added DNQX to block the contribution of HCs to the CalipHluorin response, and we carried out line scan analysis to improve temporal resolution. Resolving the small signal from noisy fluorescence measurements required signal averaging from several retinal samples. By comparing lines of cone terminals imaged immediately after a light flash (0–40 ms) with those imaged ~70–110 ms later, we could detect a small but significant delayed decrease in CalipHluorin fluorescence (n = 20 measurements for each time range, p = 0.009; Supplementary Fig. 3a,b), which was absent when the pH was buffered with HEPES (n = 20 measurements for each time range; Supplementary Fig. 3c,d). The response was transient and maximal at ~90 ms after light offset, slower than the transient acidification induced by abrupt depolarization of voltage-clamped cones (<10 ms)[20]. However, depolarization of cones following light offset is much slower than under voltage clamp, and the ensuing transient burst of vesicle release after light offset is maximal at ~100 ms[27].

Depolarizing HCs acidifies the cone synaptic cleft

To better understand how HCs regulate synaptic cleft pH, we sought a tool that would enable us to exclusively manipulate HC voltage, without affecting other retinal neurons. We generated a transgenic zebrafish line with HCs expressing a receptor not normally found in zebrafish: the invertebrate FMRFamide (Phe-Met-Arg-Phe-NH_2)-gated Na^+ channel (FaNaC)[28]. FaNaC has been used previously to depolarize genetically targeted neurons in

mammalian brain slices[29]. Expression of FaNaC in zebrafish was confined to HCs using a HC-specific connexin-55.5 promoter[11]. Crossing FaNaC and CalipHluorin transgenic lines produced fish with CalipHluorin expressed specifically in cones and FaNaC expressed specifically in HCs, as confirmed by the non-overlapping expression patterns of marker fluorescent proteins in the two cell types (Fig. 6a).

Hyperpolarization of HCs with light causes synaptic alkalinization, so we expected that depolarization of HCs by FMRFamide would lead to acidification. Indeed, in fish possessing FaNaC-expressing HCs, FMRFamide (10 μM) elicited a decrease in CalipHluorin fluorescence at cone terminals (0.585 ± 0.043, n = 5 retinas, p = 0.02; Fig. 6b, red), corresponding to acidification from a pH of 7.4 to about 6.8. In contrast, fish lacking FaNaC expression showed no change in pH from the baseline (0.984 ± 0.015, n = 4 retinas, p = 0.88; Fig. 6b, black). The FMRFamide-elicited acidification is independent of cone neurotransmitter release as the CalipHluorin response was unaltered by blocking voltage-gated Ca^{2+} channels in cones with nifedipine and AMPA receptors in HCs with GYKI-52466 (0.666 ± 0.034, n = 10 retinas, p = 0.30; Fig. 6e, gray). This indicates that the FMRFamide-elicited pH change is a direct reflection of proton flux across the HC membrane, without photoreceptors being involved.

Proton flux across the HC membrane may be mediated by proton-permeant ion channels and/or proton pumps. The vacuolar-type ATPase (V-ATPase) is a well characterized proton pump that is responsible for the acidification of synaptic vesicles and the consequent loading of neurotransmitters, including glutamate. However, physiological and immunofluorescent studies on dissociated HCs have suggested that V-ATPase is also present on the plasma membrane and can contribute to depolarization-elicited proton efflux[30]. We found that bafilomycin A1 (BFA1, 400 nM), a highly specific V-ATPase blocker, abolished the FMRFamide-elicited synaptic acidification in zebrafish retina (by ~91% of control; 0.963 ± 0.039, n = 5 retinas, p = 0.012; Fig. 6c,e, green). Washout of BFA1 restored the FMRFamide response, indicating that the V-ATPase blockade was rapidly reversible. BFA1 also reduced the light-elicited change in synaptic pH (by ~60% of control; 1.021 ± 0.004, n = 19, p = 0.001; Fig. 5d), which may be a consequence of reduced neurotransmitter release owing to impaired vesicular glutamate loading.

The invaginating tips of HC dendrites also possess connexin hemichannels[10], which are proton-permeable[31]. We found that the hemichannel blocker carbenoxolone (CBX) almost completely blocked the pH response to FMRFamide (by ~81% of control; 0.922 ± 0.047, n = 7 retinas, p = 0.004; not shown). However, patch clamp experiments on FaNaC-expressing HEK-293 cells showed that CBX directly blocks the FaNaC channel (by ~64% of control; from 3.562 ± 0.704 nA to 1.286 ± 0.341 nA, n = 7 pairs, p = 0.02), thereby interfering with the depolarizing trigger of the pH response. To circumvent this problem we used meclofenamic acid (MFA, 100 μM), a gap junction inhibitor. MFA, like CBX, affects several other types of ion channels in addition to connexin hemichannels, but MFA has no effect on FaNaC channels (Supplementary Fig. 4) and should not interfere with FMRFamide-elicited depolarization of HCs. We found that MFA had no effect on the acidification of the synaptic cleft induced by adding FMRFamide (0.617 ± 0.033, n = 10 retinas, p = 0.50; Fig. 6d,e, blue). However, it slowed dramatically the re-alkalinization

when FMRFamide was washed away (by ~78% of control; 0.224 ± 0.092, n = 6 retinas, p = 0.008; control: 1.019 ± 0.153, n = 5 retinas; Fig. 6d,f, blue). As expected, MFA greatly attenuated synaptic cleft alkalinization in response to light (by ~80% of control, 1.01 ± 0.004, n = 26, $p = 3.3*10^{-5}$; Fig. 5d). These results suggest that MFA selectively inhibits the mechanism that clears protons from the cleft while having no effect on the mechanism underlying proton efflux from HCs.

DISCUSSION

In this study, we examined the proton hypothesis of lateral inhibition by imaging an optogenetic pH indicator in the invaginating cone synapse. Previous experiments utilizing HEPES suggested that a change in synaptic pH is necessary for negative feedback to cones (for review, see Ref. 12). Other experiments involving artificial manipulation of pH showed that protons are sufficient for inhibiting cone Ca^{2+} channels and neurotransmitter release[21]. However, the possibility of non-specific actions of HEPES has left the role of protons in doubt[13]. HEPES can acidify the cytoplasm of HCs and may inhibit their connexin hemichannels whose presence is required for at least a component of lateral inhibition[13]. However, while many aminosulfonate buffers can alter intracellular pH, lateral inhibition is blocked only by the subset of compounds that buffer pH in the physiological range (*i.e.* with a pKa near 7.5)[32]. These findings are consistent with blockade being mediated by extracellular buffering *per se* rather than off-target chemical effects of aminosulfonate.

Meanwhile, the question of whether illumination naturally changes synaptic pH has remained unanswered. Our results indicate that illumination does indeed alter the extracellular pH, specifically in the synaptic cleft. Light causes synaptic alkalinization, the right direction for mediating enhancement of cone synaptic output during lateral inhibition. Moreover, within our detection limits, the change in pH appears to be of sufficient magnitude and appropriate kinetics to account for lateral inhibition.

Light-induced alkalinization can be eliminated with AMPA receptor antagonists, implicating post-synaptic cells as the signal generators of the pH change. The spatial response properties of the light-induced alkalinization point specifically to HCs. Thus, alkalinization requires summated inputs from many cones, and can occur a long lateral distance from an illuminated annulus, consistent with the circuit properties of HCs. Activation of FaNaC channels expressed exclusively in HCs provides even more definitive evidence that HCs can modulate the pH of the cone synaptic cleft.

Cone photoreceptors also release protons into the synaptic cleft as vesicles fuse with the plasma membrane, but this is a cone-autonomous process that is distinct from lateral inhibition. In fact, because of the negative feedback synapse from HCs to cones, illumination of the retina with an annulus results in an increase of vesicular release from cones in the unilluminated center. If the cone-autonomous process were dominant over the HC feedback process, one would expect to observe a net acidification of the synaptic clefts. However, we actually observed a net alkalinization, indicating that the HC-mediated process is dominant, at least under our experimental conditions.

Light causes HCs to hyperpolarize, which should drive protons down their electrochemical gradient into the cell, causing extracellular alkalinization. Likewise, depolarization of HCs, for example by FMRFamide activation of FaNaC, should lead to synaptic acidification, as we have seen in the intact retina (Fig. 6b). However, pH-selective microelectrode measurements from enzymatically dissociated HCs have revealed the opposite phenomenon; depolarization of isolated HCs can lead to extracellular alkalinization[33]. This must involve an active transporter that drives protons up their electrochemical gradient. The apparent discrepancy between these observations can be explained by active transporters and passive proton conductors co-existing in HCs, but differentially distributed across the cell. In this scenario, the HC is regionalized, with active proton transport occurring across much of the cell surface and passive proton conductors localized to the tips of HC dendrites near the cone synapse, creating microdomains of extracellular protons that are undetected by pH-sensitive microelectrodes. It is also possible that the distribution of active transporters and passive conductors had been altered by the enzymatic dissociation procedure[33], contributing to the divergent findings.

Negative feedback from HCs to cones persists indefinitely, so if protons serve as the negative feedback transmitter, their flux out of HCs must also be continuous. Over time, this would alter the proton concentration gradient across the HC plasma membrane, unless it was opposed by a compensatory active transport mechanism that maintained the gradient. A differential distribution of active transporters and passive conductors could maintain the gradient and establish a “dark current” of protons, circulating through a HC. By modulating this dark current, light-dependent hyperpolarization would change the flux of protons through open channels in invaginating synapses, thereby changing the pH of the synaptic cleft.

Our studies show that BFA1, a potent and highly specific inhibitor of V-ATPase, completely and reversibly blocks pH changes induced by changing voltage in HCs in the intact retina (Fig. 6c). This is consistent with previous pH indicator measurements from isolated HCs[30], which also showed immunocytochemical labeling for V-ATPase. V-ATPase is found in a wide variety of tissues with functional roles ranging from solute reabsorption in kidney and bone, to synaptic vesicle acidification and neurotransmitter loading in neurons. Our results indicate that V-ATPase is necessary for proton efflux from HCs, and therefore crucial for HC feedback and lateral inhibition. V-ATPase has two voltage-sensitive paths that protons can use to traverse the membrane; the coupled transport machinery involving ATP hydrolysis, and a parallel shunt that passively conducts protons down their electrochemical gradient[34]. Flux through the shunt pathway is directly related to membrane potential, and because V-ATPase is an electrogenic pump, flux through the coupled transport machinery is also voltage-sensitive.

While the V-ATPase is crucial for proton efflux and synaptic acidification, our results show that a separate mechanism that is sensitive to MFA is essential for proton influx and synaptic alkalinization (Figs. 5d and 6f). MFA is an effective and reversible blocker of connexin hemichannels[35,36], which are proton-permeant[31], highly concentrated in the dendritic tips of HCs[10], and implicated in mediating feedback using connexin mutant zebrafish (*Cx55.5*)[37]. MFA also affects several types of ion channels that are expressed in cones[38,39]. However,

FMRFamide-elicited synaptic acidification in FaNaC-expressing fish is a direct signal from HCs to the CalipHluorin pH sensor, which is unaffected by inhibiting cone synaptic transmission (Fig. 6e,f, gray). Hence, while we cannot exclude contributions from other MFA-sensitive channels in HCs, hemichannels are most likely to mediate proton influx underlying synaptic alkalinization.

The role of hemichannels in mediating proton influx and not efflux might be a consequence of the actions of intracellular protons on hemichannel gating[40,41]. Depolarization leads to intracellular acidification of HCs[33] and even a small increase in intracellular proton concentration can inhibit hemichannel opening[41]. In this scenario, the pH-dependent closure of hemichannels would allow accumulation of protons admitted into the synaptic cleft by V-ATPase during depolarization, while opening of the hemichannels after repolarization would allow protons to be retrieved from the synaptic cleft, back into the HC. HCs express several different connexins and pannexins that can heteromultimerize to form hemichannels, so genetic removal of an individual type may not be sufficient to determine which is involved in proton uptake.

While our results implicate protons as the primary mediator of HC feedback and lateral inhibition, other putative signals may play modulatory roles. It has been proposed that GABA serves as autopatic neurotransmitter in HCs and that activation of bicarbonate-permeant $GABA_A$ receptors indirectly regulates extracellular pH[42]. $GABA_A$ receptor antagonists fail to block lateral inhibition in mammalian and non-mammalian retinas[7,8], indicating that GABA release is not necessary for mediating HC feedback. However, GABA may modulate the strength of feedback, for example under different light adaptation conditions[43]. Our results also do not exclude a role for ephaptic signaling. Non-selective ion channels that conduct protons, including hemichannels, may simultaneously conduct an electrical current carried by other permeant ions that are present at higher concentrations (*e.g.* Na^+, K^+, and Cl^-), thereby generating a significant change in extracellular voltage. In this scenario, the proton mechanism and the ephaptic mechanism would operate in parallel to regulate cone neurotransmitter release. However, at least under the light stimulation conditions used in this study, the change in pH appears to be sufficient to account for negative feedback.

METHODS

Solutions

Unless indicated otherwise, the retina was perfused continuously with bicarbonate buffered saline solution containing (in mM): 100 NaCl, 2.5 KCl, 1 $MgCl_2$, 1 $CaCl_2$, 0.4 ascorbic acid, 20 glucose, 25 $NaHCO_3$, bubbled with 5% CO_2/95% O_2. For the pH/CalipHluorin intensity-titration experiment, the calibration solution contained 115 NaCl, 2.5 KCl, 1 $MgCl_2$, 1 $CaCl_2$, 20 glucose, together with 20 mM of the following respective buffers: MES for pH 5.5 and 6.5, HEPES for pH 7.5, Tris for pH 8.5 and 9.5. The buffer used in light-response experiments contained the same calibration solution plus 0.4 ascorbic acid, and 20 HEPES (Fig. 2c) or Tris (Supplementary Fig. 2c), pH 7.3. Concentrations of blockers used in Fig. 5d are DNQX: 150 μM, GYKI-52466: 50 μM, nifedipine: 100 μM, bafilomycin A1: 400 nM, meclofenamic acid: 100 μM, and carbenoxolone: 100 μM.

DNA constructs

The α2δ4 subunit of the L-type Ca^{2+} channel was cloned from zebrafish retinal RNA using RT-PCR according to sequences in GenBank *XM_691543*. A tandem sequence containing the superecliptic pHluorin (cDNA kindly provided by Dr. Richard Huganir, Johns Hopkins University School of Medicine), a protease recognition site, and a 15-amino acid linker, was inserted between the predicted signal peptide and the coding sequence of the α2δ4 subunit. The resulting construct was cloned into vector *pDONR221* (Invitrogen) to produce *pME-CalipHluorin*. Gateway® recombination cloning (Invitrogen) with *p5E-TαCP* (kindly provided by Susan Brockerhoff, University of Washington), *pME-CalipHluorin*, and *p3E-MTpA* and *pDestTol2CG2* from the Tol2kit[44] was used for generating the CalipHluorin construct for expression in zebrafish. For transfecting rat hippocampal neurons (Supplementary Fig. 1), a different plasmid was assembled from *p5E-βactin2* (Tol2kit), *pME-CalipHluorin*, *p3E-MTpA* and *pDestTol2pA2* (Tol2kit).

The invertebrate FMRFamide-gated Na^+ channel (FaNaC) from *Helix aspersa* (EMBL accession number *X92113*) was subcloned from the vector *pCMVTnT/FaNaC*[29] (kindly provided by Dr. McQuiston, VCU School of Medicine) into *pDONR221* to obtain *pME-FaNaC*. For bicistronic expression of FaNaC with the red fluorescent protein, mCherry, the coding sequence of the viral 2A peptide (GSGATNFSLLKQAGDVEENPGP)[45] was inserted at the 5′-end of the mCherry coding sequence in *p3E-mCherrypA*[44] to produce *p3E-2AmCherry*. To generate the FaNaC constructs, we recombined *p5E-Cx55.5*[11] (kindly provided by Dr. Kamermans, Netherlands Institute for Neuroscience), *pME-FaNaC*, *p3E-2AmCherry*, and *pDestTol2CG2* from the Tol2kit for making transgenic fish, and *p5E-CMV* (Tol2kit), *pME-ME-FaNaC*, *p3E-2AmCherry* and *pDestTol2pA2* (Tol2kit) for transfecting HEK-293 cells (Supplementary Fig. 4).

Cell culture

HEK-293 cells were cultured under standard conditions. Cells were plated on poly L-lysine (0.1 mg/ml)-coated coverslips at a density of 13000 cells/cm^2 for electrophysiological measurements. HEK-293 cells were transfected with the *pCMV-FaNaC-2A-mCherry* construct using calcium phosphate precipitation and measured 2–4 days after transfection. FaNaC-positive cells were identified by their mCherry fluorescence.

Electrophysiology

Patch clamp recordings of HEK-293 cells (Supplementary Fig. 4) were performed at room temperature in voltage-clamp mode. External bath solution contains (in mM) 138 NaCl, 1.5 KCl, 1.2 $MgCl_2$, 2.5 $CaCl_2$, 5 HEPES and 10 glucose. Pipette solution contains 30 NaCl, 100 CsCl, 10 HEPES, 2 $MgCl_2$, 1 $CaCl_2$, 2 MgATP, 0.05 NaGTP, 10 EGTA and 5 glucose. All solutions were adjusted to pH 7.4. Drugs were applied through a perfusion line and the pipette tip was placed in close proximity to the recorded cell. Electrophysiological measurements were performed with a Patch-Clamp PC501A amplifier (Warner) and recorded using pClampex 10.1 software (Molecular Devices). Pipette resistance was 3~6 MΩ. Voltage clamp recordings were low-pass filtered at 2 kHz. Data were analyzed using Clampfit 10.2 (Molecular Devices) and MATLAB® (MathWorks).

Transgenic fish

One or two-cell stage zebrafish (AB strain) embryos were microinjected with the *CalipHluorin* or *FaNaC* DNA construct together with *Tol2* mRNA for higher germline transmission rate[44]. The transgene-positive F0 founders were selected by screening for green heart fluorescence in 2–4 dpf embryos[44], and raised at 28.5°C in a 14/10 hrs light/dark cycle. The adult F0 fish were inbred and their transgene-positive progeny were raised and used for imaging experiments. To generate CalipHluorin/FaNaC double transgenic fish, the CalipHluorin transgenic fish line was crossed with the FaNaC fish line. The genotype was verified by PCR.

Tissue preparation

All procedures were approved by the UC Berkeley Animal Care and Use Committee. After adult fish were euthanized in MS-222, the dark-adapted retinas were isolated from the eyecups with the RPE removed, and kept in darkness in bubbled bicarbonate buffered saline. For flat-mount preparation, retinas were mounted onto a Biopore™ membrane (MILLIPORE) with photoreceptors facing the membrane[46]. For slice preparation, retinas were mounted onto nitrocellulose filter paper (pore size 0.8 μm, MILLIPORE) with retinal ganglion cells facing the paper. Retinas were sliced to 200 μm in thickness using a tissue slicer[27]. Slices were counter-stained with 2.5 μM sulforhodamine 101 for Fig. 1c. For Supplementary Fig. 1, hippocampal neurons were prepared and transfected using standard protocols.

Image acquisition

The flat-mount retina was moved to the imaging chamber with photoreceptor side facing the glass bottom of the chamber. We used a custom-built microscope based on a design from the Karel Svoboda lab (Janelia Farm Research Campus, HHMI) equipped with a Ti:Sapphire pulse laser (Coherent) tuned to 910 nm. The microscope was controlled by ScanImage r3.6 software[47] with plugins developed in our lab. For light stimulation experiments, an area of 30×30 μm^2 was imaged at a frame rate of 128 ms/frame and binned into 64×64-pixel images. The high magnification image in Fig. 1g was deconvolved using the Richardson-Lucy algorithm to enhance the sharpness of the image.

To image CalipHluorin and mCherry fluorescence at the same time (Fig. 6a), we used a Zeiss LSM710 equipped with a spectral analyzer. CalipHluorin was excited at 488 nm and mCherry was excited at 561 nm.

Light stimulation

The light source is a LUXEON® Rebel Blue LED (PHILIPS) shortpass-filtered at 460 nm and a LUXEON® Rebel Amber LED longpass-filtered at 550 nm. Light from the 2 LEDs was combined with a 505 nm-longpass dichroic mirror, and coupled to the projection optics with an optical fiber. The green portion of the spectrum (from 460 to 550 nm) was filtered out to protect the photomultiplier from photodamage. Except for Fig. 5a (light intensity vs. F/F_0), we used a light intensity of 10^{18}–10^{19} photons/m^2/s[(48)], measured with a photometer at the specimen plane. A pattern mask (*e.g.* a spot or an annulus) was placed in the

projection light and projected onto the retina through the condenser. A program written in MATLAB® (MathWorks) was used to command the shutter (TS6B, UNIBLITZ®) for controlling flash duration. Except for Fig. 4a (light duration vs. F/F_0), flash duration of 508 ms was used. Light stimulation was given at ~1 s after the beginning of a scan series, and repeated 3 times (Supplementary Fig. 5b, black/yellow bar) in each experimental run.

For measuring the intensity vs. response relation (Fig. 5a), we used a single blue LED, shortpass filtered through a 460 nm filter, rather than the mixed blue-amber LEDs. This enabled more accurate estimation of the projected light intensity. The spectral sensitivity of zebrafish opsins is blue-shifted[49], thus this light should stimulate all except the long-wavelength cones. The intensity of the stimulation light was modulated by changing the brightness of the LED combined with different neutral density filters (THORLABS).

Image analysis

We first selected a region of interest (ROI) from the cone terminal image. The ROI was generated in ImageJ (rsbweb.nih.gov/ij) using a thresholding-based technique (Supplementary Fig. 5a, red lines). We excluded from the ROI the first row of pixels (*i.e.* the first 2 ms of the scanned image), collected after terminating the light flash, to avoid detecting afterglow of the stimulation light. The background signal, measured at the end of the experiment in the absence of laser scanning, was subtracted from each image. To estimate photobleaching, the average pixel intensity within the ROI of each frame (termed F) was fitted with a single-exponential function $y = ae^{-bx}$, where x is the frame number and y is the intensity (Supplementary Fig. 5b, red line). Fluorescence intensities acquired during the light flash were excluded from the photobleach fitting routine because they were confounded with the stimulus light (Fig. 2a, gray arrowheads). The CalipHluorin response decays within 6 frames after a light flash (~750 ms), so data from these time points were also excluded from the fitting routine. To compensate for photobleaching, the original intensity (F) of each frame was divided by its corresponding value in the fitted curve (y). The compensated light responses from the 3 flashes were aligned and the mean response was calculated, and defined as n of 1 (Supplementary Fig. 5c).

For line scan analysis (Supplementary Fig. 3), since each image (30 μm square) is composed of 64 raster-scanned lines acquired at a speed of 2 ms/line, the fluorescence intensity in each line encodes the pH value of a designated time point which is 2 ms apart from each other. As a result, the same line in two consecutive frames represents time points that are 128 ms apart. Photobleaching compensation and fluorescence normalization described previously was applied to data grouped from each single line. The compensated/normalized fluorescence intensities from each line were assembled, which resemble the pH response at 2 ms temporal resolution.

Statistical analysis and curve fitting

Statistical significance of Fig. 6e,f and Supplementary Fig. 4 (sample number <10) was determined by two-sided non-parametric Mann-Whitney U-test, all others were determined by two-tailed Student's t-test. Data points and error bars represent mean ± SEM. In Fig. 3b, each data set was fitted with equation $y = y_0 + y_{max} / (1 + 10^{(pKa - pH)})$[14], where y is the

fluorescence intensity, y_0 is the baseline, y_{max} is the magnitude of maximal response, and *pKa* is the logarithm of the equilibrium constant for protonation. The data set was then normalized (*i.e.* $(y - y_0) / y_{max}$), and pooled together with other sets of experiments. The combined data sets were averaged and fitted with the same equation again to yield the final fitted curve (Fig. 3b, gray).

For Fig. 3c, the fluorescence intensity at pH 7.6 was normalized to the intensity at pH 7.4 (*i.e.* $F_{pH7.6}/F_{pH7.4}$) in each set of experiment. Linear interpolation of the average ratio of $F_{pH7.6}/F_{pH7.4}$ (Fig. 3c, gray) was used to calculate the estimated pH values in the dark and light. The *y* axis of Fig. 3c was converted to relative ΔF from the dark for clearer representation.

The decay of the CalipHluorin signal in Fig. 4c (0.5 s) was fitted with a single-exponential function $y = y_0 + y_{max}e^{-kx}$, where *x* is time after light flash, *y* is the magnitude of light response, y_0 is the baseline, y_{max} is the magnitude of maximal response, and *k* determines the speed of the decay. The first data point after light flash, which deviated from expected exponential decay, was excluded from the fit.

In Fig. 5a, relative light responses (*i.e.* F/F_0) from data sets obtained at different light intensities were combined and fitted with equation $y = y_0 + y_{max} \times x^n / (x^n + K^n)$[50], where *x* is the light intensity, *y* is the magnitude of light response, y_0 is the baseline, y_{max} is the magnitude of maximal response, *K* is the intensity needed to elicit half-maximal of the light response, and *n* is the slope factor.

Supplementary Material

Refer to Web version on PubMed Central for supplementary material.

Acknowledgments

We thank Rachel Montpetit for help with molecular biology, Jeffrey LeDue for help with optical instrumentation, Dr. Wallace Thoreson for helpful discussions, Dr. Christopher Davenport for critical reading of the manuscript, and Drs. Susan Brockerhoff, Richard Huganir, Maarten Kamermans, and A. Rory McQuiston for providing plasmids. This work was supported by grants from the National Institutes of Health to R.H.K. (R01EY018957 and P30EY003176) and T.M.W. (F32EY020095).

References

1. Baylor DA, Fuortes MG, O'Bryan PM. Receptive fields of cones in the retina of the turtle. J Physiol. 1971; 214:265–94. [PubMed: 5579638]
2. Copenhagen DR, Jahr CE. Release of endogenous excitatory amino acids from turtle photoreceptors. Nature. 1989; 341:536–9. [PubMed: 2477707]
3. Verweij J, Kamermans M, Spekreijse H. Horizontal cells feed back to cones by shifting the cone calcium-current activation range. Vision Res. 1996; 36:3943–53. [PubMed: 9068848]
4. Babai N, Thoreson WB. Horizontal cell feedback regulates calcium currents and intracellular calcium levels in rod photoreceptors of salamander and mouse retina. J Physiol. 2009; 587:2353–64. [PubMed: 19332495]
5. Schwartz EA. Calcium-independent release of GABA from isolated horizontal cells of the toad retina. J Physiol. 1982; 323:211–27. [PubMed: 6808119]
6. Kaneko A, Tachibana M. Effects of gamma-aminobutyric acid on isolated cone photoreceptors of the turtle retina. J Physiol. 1986; 373:443–61. [PubMed: 3746679]

7. Thoreson WB, Burkhardt DA. Effects of synaptic blocking agents on the depolarizing responses of turtle cones evoked by surround illumination. Vis Neurosci. 1990; 5:571–83. [PubMed: 2085473]
8. Verweij J, Hornstein EP, Schnapf JL. Surround antagonism in macaque cone photoreceptors. J Neurosci. 2003; 23:10249–10257. [PubMed: 14614083]
9. Byzov AL, Shura-Bura TM. Electrical feedback mechanism in the processing of signals in the outer plexiform layer of the retina. Vision Res. 1986; 26:33–44. [PubMed: 3012877]
10. Kamermans M, et al. Hemichannel-mediated inhibition in the outer retina. Science. 2001; 292:1178–80. [PubMed: 11349152]
11. Shields CR, et al. Retinal horizontal cell-specific promoter activity and protein expression of zebrafish connexin 52.6 and connexin 55.5. J Comp Neurol. 2007; 501:765–79. [PubMed: 17299759]
12. Hirasawa H, Yamada M, Kaneko A. Acidification of the synaptic cleft of cone photoreceptor terminal controls the amount of transmitter release, thereby forming the receptive field surround in the vertebrate retina. J Physiol Sci. 2012; 62:359–375. [PubMed: 22773408]
13. Fahrenfort I, et al. Hemichannel-mediated and pH-based feedback from horizontal cells to cones in the vertebrate retina. PLoS One. 2009; 4:e6090. [PubMed: 19564917]
14. Sankaranarayanan S, De Angelis D, Rothman JE, Ryan TA. The use of pHluorins for optical measurements of presynaptic activity. Biophys J. 2000; 79:2199–208. [PubMed: 11023924]
15. Kennedy BN, et al. Identification of a zebrafish cone photoreceptor-specific promoter and genetic rescue of achromatopsia in the nof mutant. Invest Ophthalmol Vis Sci. 2007; 48:522–9. [PubMed: 17251445]
16. Tom Dieck S, et al. Molecular dissection of the photoreceptor ribbon synapse: physical interaction of Bassoon and RIBEYE is essential for the assembly of the ribbon complex. J Cell Biol. 2005; 168:825–36. [PubMed: 15728193]
17. Li YN, Matsui JI, Dowling JE. Specificity of the horizontal cell-photoreceptor connections in the zebrafish (Danio rerio) retina. J Comp Neurol. 2009; 516:442–53. [PubMed: 19655401]
18. Euler T, et al. Eyecup scope–optical recordings of light stimulus-evoked fluorescence signals in the retina. Pflugers Arch. 2009; 457:1393–414. [PubMed: 19023590]
19. Hirasawa H, Kaneko A. pH changes in the invaginating synaptic cleft mediate feedback from horizontal cells to cone photoreceptors by modulating Ca2+ channels. J Gen Physiol. 2003; 122:657–71. [PubMed: 14610018]
20. DeVries SH. Exocytosed protons feedback to suppress the Ca2+ current in mammalian cone photoreceptors. Neuron. 2001; 32:1107–17. [PubMed: 11754841]
21. Barnes S, Merchant V, Mahmud F. Modulation of transmission gain by protons at the photoreceptor output synapse. Proc Natl Acad Sci USA. 1993; 90:10081–5. [PubMed: 7694280]
22. Piccolino M. Chapter 6 Horizontal cells: Historical controversies and new interest. Prog Retin Res. 1986; 5:147–163.
23. Yang XL, Tornqvist K, Dowling JE. Modulation of cone horizontal cell activity in the teleost fish retina. I Effects of prolonged darkness and background illumination on light responsiveness. J Neurosci. 1988; 8:2259–68. [PubMed: 3249224]
24. Daniels BA, Baldridge WH. The light-induced reduction of horizontal cell receptive field size in the goldfish retina involves nitric oxide. Vis Neurosci. 2011; 28:137–44. [PubMed: 21324227]
25. Wilkinson MF, Barnes S. The dihydropyridine-sensitive calcium channel subtype in cone photoreceptors. J Gen Physiol. 1996; 107:621–30. [PubMed: 8740375]
26. Klooster J, Studholme KM, Yazulla S. Localization of the AMPA subunit GluR2 in the outer plexiform layer of goldfish retina. J Comp Neurol. 2001; 441:155–67. [PubMed: 11745642]
27. Jackman SL, Babai N, Chambers JJ, Thoreson WB, Kramer RH. A positive feedback synapse from retinal horizontal cells to cone photoreceptors. PLoS Biol. 2011; 9:e1001057. [PubMed: 21559323]
28. Lingueglia E, Champigny G, Lazdunski M, Barbry P. Cloning of the amiloride-sensitive FMRFamide peptide-gated sodium channel. Nature. 1995; 378:730–3. [PubMed: 7501021]

29. Schanuel SM, Bell KA, Henderson SC, McQuiston AR. Heterologous expression of the invertebrate FMRFamide-gated sodium channel as a mechanism to selectively activate mammalian neurons. Neuroscience. 2008; 155:374–86. [PubMed: 18598740]
30. Jouhou H, et al. Depolarization of isolated horizontal cells of fish acidifies their immediate surrounding by activating V-ATPase. J Physiol. 2007; 585:401–12. [PubMed: 17932147]
31. Zaniboni M, et al. Proton permeation through the myocardial gap junction. Circ Res. 2003; 93:726–35. [PubMed: 12958146]
32. Trenholm S, Baldridge WH. The effect of aminosulfonate buffers on the light responses and intracellular pH of goldfish retinal horizontal cells. J Neurochem. 2010; 115:102–11. [PubMed: 20633206]
33. Jacoby J, et al. Extracellular pH dynamics of retinal horizontal cells examined using electrochemical and fluorometric methods. J Neurophysiol. 2012; 107:868–79. [PubMed: 22090459]
34. Kettner C, Bertl A, Obermeyer G, Slayman C, Bihler H. Electrophysiological analysis of the yeast V-type proton pump: variable coupling ratio and proton shunt. Biophys J. 2003; 85:3730–3738. [PubMed: 14645064]
35. Pan F, Mills SL, Massey SC. Screening of gap junction antagonists on dye coupling in the rabbit retina. Vis Neurosci. 2007; 24:609–618. [PubMed: 17711600]
36. Liu X, Hashimoto-Torii K, Torii M, Ding C, Rakic P. Gap junctions/hemichannels modulate interkinetic nuclear migration in the forebrain precursors. J Neurosci. 2010; 30:4197–4209. [PubMed: 20335455]
37. Klaassen LJ, et al. Synaptic transmission from horizontal cells to cones is impaired by loss of connexin hemichannels. PLoS Biol. 2011; 9:e1001107. [PubMed: 21811399]
38. Peretz A, et al. Meclofenamic acid and diclofenac, novel templates of KCNQ2/Q3 potassium channel openers, depress cortical neuron activity and exhibit anticonvulsant properties. Mol Pharmacol. 2005; 67:1053–1066. [PubMed: 15598972]
39. Liantonio A, et al. Niflumic acid inhibits chloride conductance of rat skeletal muscle by directly inhibiting the CLC-1 channel and by increasing intracellular calcium. Br J Pharmacol. 2007; 150:235–247. [PubMed: 17128287]
40. Spray DC, Harris AL, Bennett MV. Gap junctional conductance is a simple and sensitive function of intracellular pH. Science. 1981; 211:712–715. [PubMed: 6779379]
41. Trexler EB, Bukauskas FF, Bennett MV, Bargiello TA, Verselis VK. Rapid and direct effects of pH on connexins revealed by the connexin46 hemichannel preparation. J Gen Physiol. 1999; 113:721–742. [PubMed: 10228184]
42. Liu X, Hirano AA, Sun X, Brecha NC, Barnes S. Calcium channels in rat horizontal cells regulate feedback inhibition of photoreceptors through an unconventional GABA- and pH-sensitive mechanism. J Physiol (Lond). 2013; 591:3309–3324. [PubMed: 23613534]
43. Wu SM. Feedback connections and operation of the outer plexiform layer of the retina. Curr Opin Neurobiol. 1992; 2:462–468. [PubMed: 1525544]
44. Kwan KM, et al. The Tol2kit: a multisite gateway-based construction kit for Tol2 transposon transgenesis constructs. Dev Dyn. 2007; 236:3088–99. [PubMed: 17937395]
45. Provost E, Rhee J, Leach SD. Viral 2A peptides allow expression of multiple proteins from a single ORF in transgenic zebrafish embryos. Genesis. 2007; 45:625–9. [PubMed: 17941043]
46. Koizumi A, Zeck G, Ben Y, Masland RH, Jakobs TC. Organotypic culture of physiologically functional adult mammalian retinas. PLoS ONE. 2007; 2:e221. [PubMed: 17311097]
47. Pologruto TA, Sabatini BL, Svoboda K. ScanImage: flexible software for operating laser scanning microscopes. Biomed Eng Online. 2003; 2:13. [PubMed: 12801419]
48. Davenport CM, Detwiler PB, Dacey DM. Effects of pH buffering on horizontal and ganglion cell light responses in primate retina: evidence for the proton hypothesis of surround formation. J Neurosci. 2008; 28:456–64. [PubMed: 18184788]
49. Chinen A, Hamaoka T, Yamada Y, Kawamura S. Gene duplication and spectral diversification of cone visual pigments of zebrafish. Genetics. 2003; 163:663–75. [PubMed: 12618404]
50. Joselevitch C, Kamermans M. Interaction between rod and cone inputs in mixed-input bipolar cells in goldfish retina. J Neurosci Res. 2007; 85:1579–91. [PubMed: 17342779]

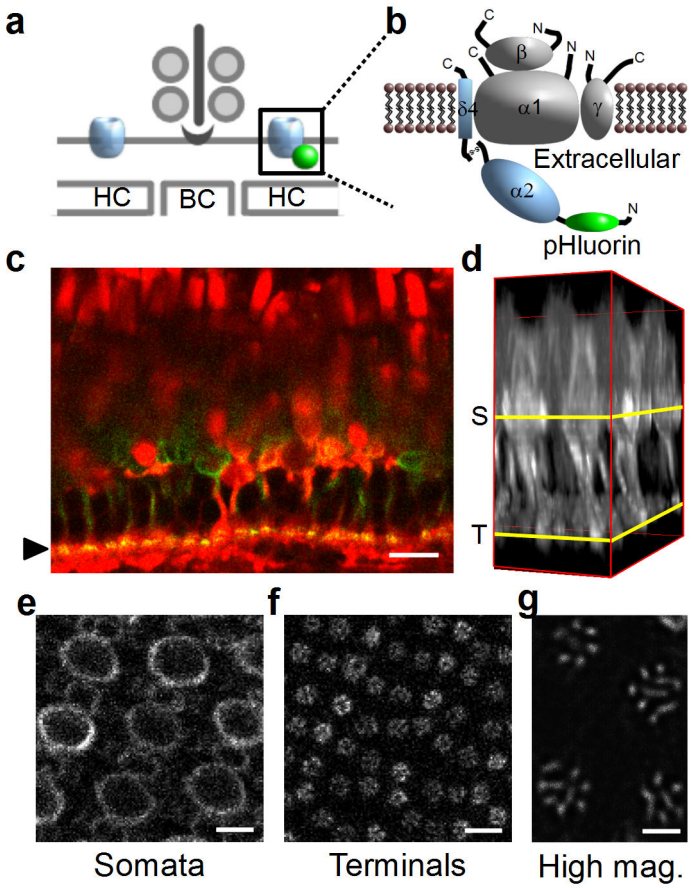

Figure 1.

Design and expression of CalipHluorin, a genetically engineered fluorescent pH sensor. (**a**) Schematic diagram of the cone synapse with CalipHluorin localized to cone terminals, near ribbon synapse contacts with horizontal cells (HC) and bipolar cell (BC). (**b**) To produce CalipHluorin, the pH-sensitive GFP, pHluorin, was fused to the extracellular N-terminus of the α2δ4 subunit of the Ca^{2+} channel. (**c**)-(**g**) Images, obtained with 2-photon microscopy, of retinas from transgenic zebrafish expressing CalipHluorin. (**c**) A retinal slice shows expression of CalipHluorin (green) in the somata and terminals (arrowhead) of cones. The slice was counter-stained with sulforhodamine 101 (red). (**d**) A 3D reconstruction of CalipHluorin fluorescence from optical sections through the photoreceptor and outer plexiform layers of a flat-mounted retina. Optical sections corresponding to somata (S) and terminals (T) are shown in (**e**) and (**f**). In (**c**), the largest somata (UV cones) are interleaved with smaller somata (blue cones). (**g**) Higher magnification image of cone terminals expressing CalipHluorin. Scale bars in (**c**), 10 μm; (**e**), (**f**), 5 μm; (**g**), 2 μm.

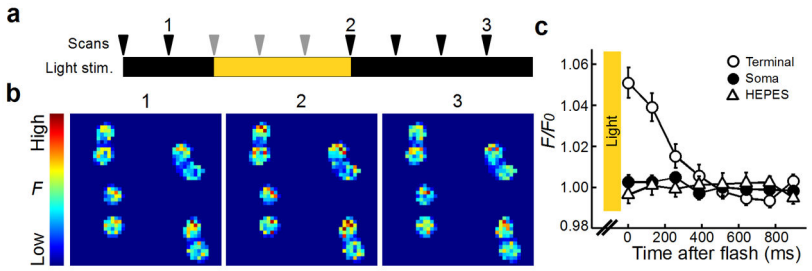

Figure 2.

Light induces alkalization of the cone synaptic cleft. (**a**) Timeline of the experimental protocol. Scans were collected at a constant interval (arrowheads). Frames that were acquired during the light flash (gray arrowheads) were confounded with the simulation light and therefore excluded from the analysis routine. (**b**) Images of cone terminals collected before a light flash (1), immediately after the flash (2), and ~1 s after the flash (3). Fluorescence intensity (color-coded according to the scale bar on the left) was brightest immediately after the light flash (note the increase in red pixels). (**c**) Full-field illumination for 0.5 s caused a 5% increase in average pixel intensity at the terminals (n = 23) but not at the soma (n = 20, $p = 1.7*10^{-6}$). The increase in fluorescence was blocked by addition of HEPES (n = 21, $p = 2.7*10^{-7}$). Data are mean ± s.e.m..

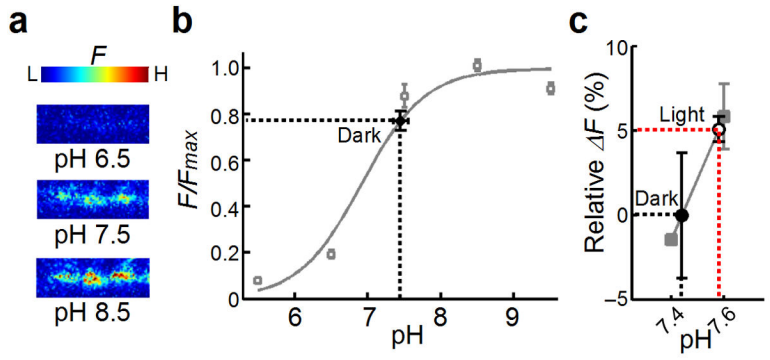

Figure 3.

Quantification of the light-induced change in pH. (**a**) The effect of changing extracellular pH on the CalipHluorin fluorescence of cone terminals in a retinal slice. (**b**) Calibration of the relationship between pH and fluorescence. From the fitted curve (solid line), the resting (*i.e.* dark) pH at cone terminals is estimated at ~7.4 (filled circle, $n = 4$). (**c**) More precise calibration in the physiological range of extracellular pH ($n = 6$). The CalipHluorin fluorescence in darkness (black circle) is slightly greater than in solution buffered to pH 7.4 (gray square). The CalipHluorin fluorescence after a light flash (open circle) is slightly less than in solution buffered to pH 7.6 (gray square). From this calibration, the change in fluorescence from darkness to light corresponds to alkalinization of 0.14 pH unit (from black to red dotted lines). The fluorescence was normalized to the value in pH 7.4. Data are mean ± s.e.m..

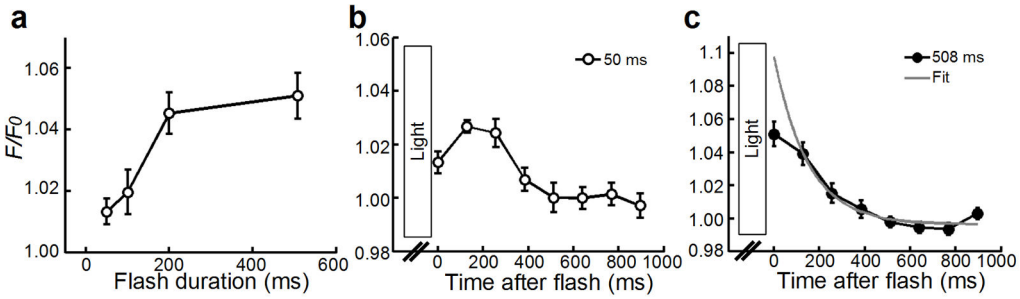

Figure 4.

The temporal properties of the pH change resemble those of the HC light response. (**a**) The pH response increases with flash duration, up to 0.5 s. (**b**) After a brief flash, the pH signal continues to rise after light offset (**c**) The pH response after the prolonged flash (black) was well-fit by a single exponential decay (gray), except for the earliest time point where the pH was lower than expected. Data are mean ± s.e.m..

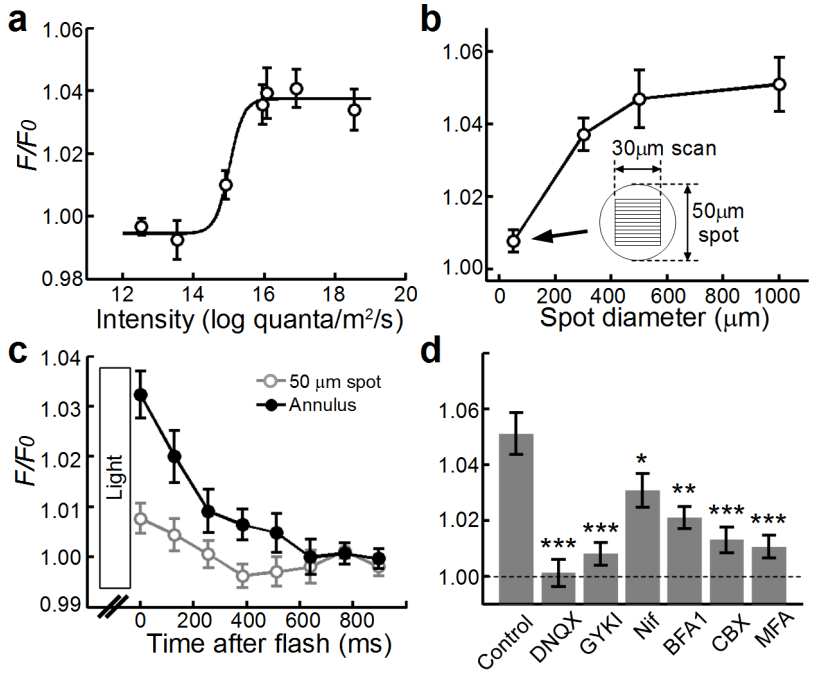

Figure 5.

The spatial and pharmacological features of the pH change match those of the HC light response. (**a**) The pH response was steeply dependent on light intensity, within the mid-photopic range. (**b**) The pH response grew larger with spot diameter up to 500 μm. (**c**) The pH response can be driven by surround illumination exclusively. A large pH change was elicited by an annulus of light (300/1000 μ inner/outer diameter) that excluded imaged area (a 30 μm square). A small spot of light (50 μm diameter) covering the entire imaged area elicited a much smaller response. (**d**) The pH signal in response to DNQX (n = 21, p = 2.1*10^{-6}), GYKI-52466 (n = 21, p = 1.3*10^{-5}), nifedipine (Nif, n = 25, p = 0.038), bafilomycin A1 (BFA1, n = 19, p = 0.001), carbenoxolone (CBX, n = 25, p = 1.1*10^{-4}), and meclofenamic acid (MFA, n = 26, p = 3.3*10^{-5}) is shown. *, p < 0.05. **, p < 0.01. ***, p < 0.001. Data are mean ± s.e.m..

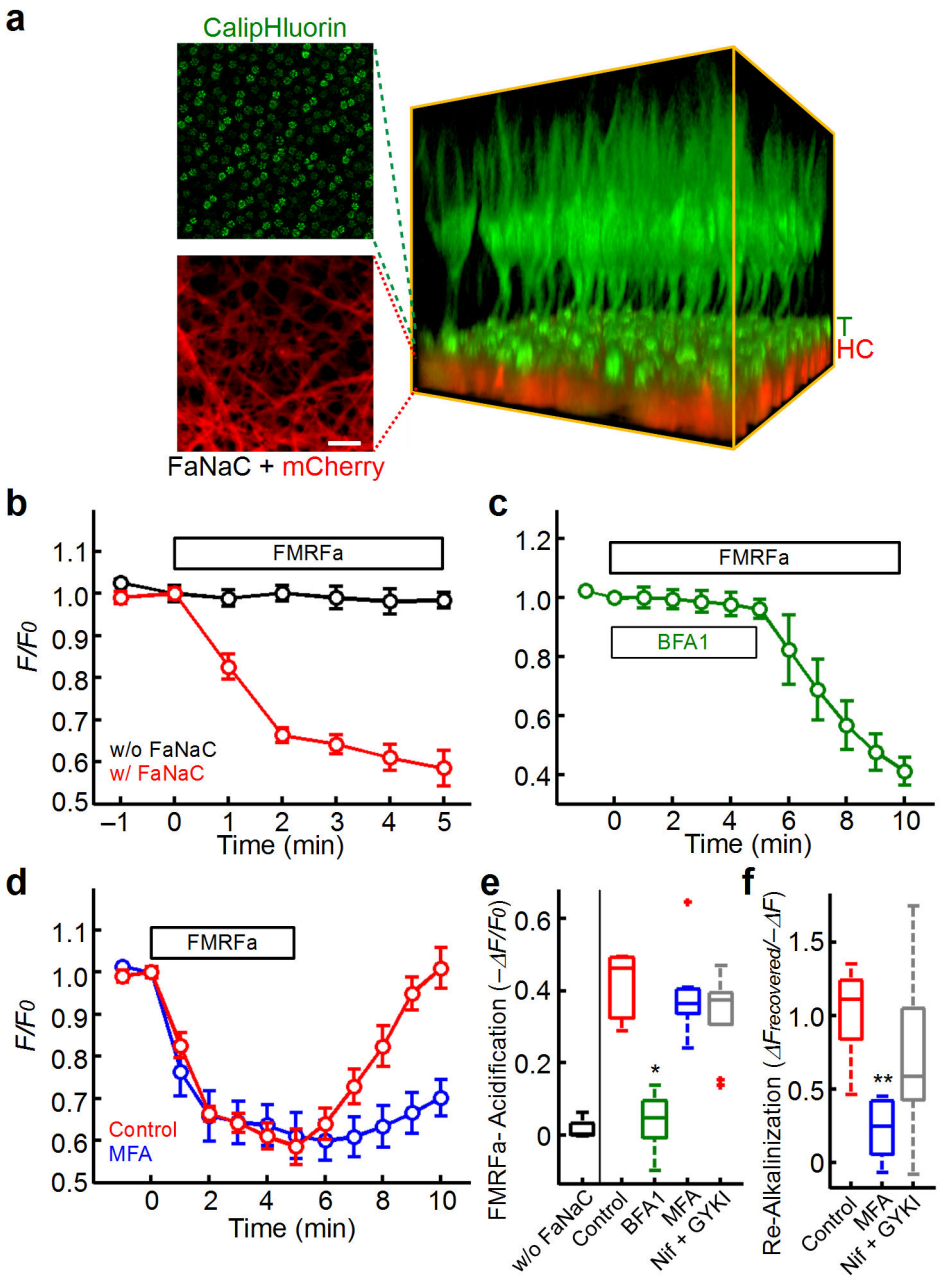

Figure 6.

Activation of an exogenously expressed ligand-gated Na^+ channel in HCs acidifies the cone synaptic cleft. (**a**) Double transgenic fish carrying CalipHluorin (green) in cones and FaNaC + mCherry (red) in horizontal cells (HC). Optical sections (left) and a 3D reconstruction (right) showing cone terminals (T) adjacent to the HC layer. (**b**) FMRFamide (FMRFa) caused a decrease in CalipHluorin fluorescence in retinas from the double transgenic fish (red, $n = 5$, $p = 0.02$), but not in the retina from the CalipHluorin-only fish (black, $n = 4$, $p = 0.88$). (**c**)–(**e**) The synaptic acidification mediated by activation of FaNaC in HCs was significantly reduced by the V-ATPase blocker BFA1 (100 μM, green, $n = 5$, $p = 0.012$), but not by the hemichannel inhibitor MFA (100 μM, blue, $n = 6$ for **d**, $n = 10$ for **e**, $p = 0.50$).

However, MFA significantly slowed the re-alkalinization of synaptic pH after washing out FMRFamide from the retina (**d** and **f**, blue, $n = 6$, $p = 0.008$). Adding nifedipine and GYKI-52466 did not significantly affect FMRFamide-elicited acidification (**e**, gray, $n = 10$, $p = 0.30$) or the re-alkalinization after washing out FMRFamide (**f**, gray, $n = 6$, $p = 0.24$). The average decrease of CalipHluorin fluorescence 5 min after FMRFamide is plotted in (**e**); the recovery of fluorescence 5 min after FMRFamide washout is plotted in (**f**). Scale bars in (**a**), 10 μm. *, $p < 0.05$. **, $p < 0.01$. (**b**)–(**d**) Data are mean ± s.e.m.. Box-whisker plots in (**e**) and (**f**) represent the first three quartiles (25%, median and 75%) and values 1.5× the interquartile range below the first quartile (lower horizontal line) and above the third quartile (upper horizontal line) and data points beyond the whiskers are displayed using +.